Dielectric response function and plasmon dispersion in a strongly coupled two-dimensional Coulomb liquid

Kenneth I. Golden* and Hania Mahassen
Department of Mathematics and Statistics, University of Vermont, Burlington, Vermont 05405, USA

Gabor J. Kalman
Department of Physics, Boston College, Chestnut Hill, Massachusetts 02467, USA
(Received 2 April 2004; published 30 August 2004)

We have formulated a dielectric response function for strongly coupled two-dimensional Coulomb liquids in the $T=0$ quantum domain. The formulation is based on the classical quasilocalized charge approximation [G. Kalman and K. I. Golden, Phys. Rev. A **41**, 5516 (1990); K. I. Golden and G. Kalman, Phys. Plasmas **7**, 14 (2000)] and extends the QLCA formalism into the quantum domain. We calculate the dispersion of the longitudinal plasmon mode for $r_s=10$, 20, 40 and the resulting dispersion curves are compared with recent experimental results. We also conjecture the possible existence of a new high-wave-number collective excitation in close proximity to the right boundary of the pair continuum.

DOI: 10.1103/PhysRevE.70.026406 PACS number(s): 52.27.Gr, 52.25.Mq, 73.20.Mf

I. INTRODUCTION

This paper addresses the problem of longitudinal collective mode dispersion in strongly coupled two-dimensional (2D) Coulomb liquids at zero temperature. The 2D Coulomb liquid is modeled as a one-component plasma (OCP) in which charged particle motions in a uniform rigid neutralizing background are restricted to a plane having zero thickness and large but bounded area A. The $N(=nA)$ charges interact via the $\phi_{2D}(r)=e^2/\varepsilon_s r$ Coulomb potential, r being the in-plane separation distance and ε_s the dielectric constant of the substrate; $\phi_{2D}(q)=2\pi e^2/(\varepsilon_s q)$ is its Fourier transform. In the zero-temperature quantum domain, the customary measure of the coupling strength is $r_s=a/a_B$, where $a=1/\sqrt{\pi n}$ is the Wigner-Seitz radius and $a_B=\varepsilon_s\hbar^2/(me^2)$ is the effective Bohr radius; $\varepsilon_F=\pi n\hbar^2/m$ is the Fermi energy of the noninteracting 2D electron gas and $k_F=\sqrt{2\pi n}$ is the 2D Fermi wave number.

The important question of the dynamics of strong Coulomb interactions and how they affect the dispersion of collective modes in strongly coupled 2D Coulomb liquids is one that has received a great deal of attention primarily from theorists [1–15] over the past three decades. Interest in this problem is further intensified by recent inelastic light scattering experiments [16,17] that, for the first time, provide measurements of plasmon dispersion in ultralow density 2D electron systems in GaAs quantum wells at finite temperatures.

In the high-temperature classical (CL) domain, theoretical calculations of the dielectric function, $\varepsilon(\mathbf{q},\omega)$, and dispersion and damping of the collective modes have been carried out [CL(i)] by following a microscopic hydrodynamic approach [2], [CL(ii)] by adapting the conventional three-dimensional (3D) Singwi-Tosi-Land-Sjolander (STLS) [18] mean-field-theory approach to the 2D OCP [3], [CL(iii)] by an approximation scheme that combines the quadratic fluctuation-dissipation theorem with linearized moment equations featuring three-point dynamical structure functions [5], [CL(iv)] by adapting the quasilocalized charge approximation (QLCA) approach [11,19] to the 2D OCP [7], and [CL(v)] by adapting the velocity-average-approximation (VAA) approach [20] to the 2D OCP in the weakly degenerate quantum domain [12]. Computer-generated data pertaining to the dynamical structure function and collective mode dispersion in the strongly coupled 2D classical OCP liquid have been available since 1980 thanks to the molecular dynamics (MD) simulations of Totsuji and Kakeya [21] and more recently by Kalman *et al.* [22].

In the zero-temperature quantum (Q) domain, a variety of approaches have been used as well for the calculation of the 2D dielectric response function and plasmon dispersion: [Q(i)] At long-wavelengths ($q\to 0$), the plasmon dispersion has been inferred by supposing that it is sufficient to replace $\varepsilon(\mathbf{q},\omega)$ by its high-frequency sum rule expansion [4]. More elaborate approaches have built on the concept of the local field factor $G(\mathbf{q},\omega)$. For finite-q values, [Q(ii)] an early approximation for the static $G(\mathbf{q})$, due to Hubbard and Jonson [1], was $G_H(\mathbf{q})=q/(2\sqrt{q^2+k_F^2})$. A more sophisticated static local field correction has been formulated [Q(iii)] by adapting the classical STLS approach [18] to the 2D quantum electron liquid [1,8,9]. Dynamical local field factors have been formulated [Q(iv)] via a 2D quantum kinetic equation treatment using a Mori memory function formalism that takes account of the dynamics of the exchange-correlation hole surrounding each electron [6], and [Q(v)] by adapting a quantum mechanical version [23] of the STLS theory (the "qSTLS") to the 2D Coulomb liquid at zero temperature [10].

At finite temperatures, motivated by the recent inelastic light scattering experiments of Eriksson *et al.* [16] and Hirjibehedin *et al.* [17], Hwang and Das Sarma [13] proposed a simple theoretical model for the calculation of 2D plasmon dispersion. Based on the premise that finite temperature and

*Also at Department of Physics, University of Vermont, Burlington, Vermont 05405, USA. Email address: golden@emba.uvm.edu

correlation effects tend to cancel each other, Hwang and Das Sarma suppose that the local field correction can be reasonably well represented by the finite-temperature 2D Hubbard approximation $G_H(\mathbf{q},T)=q/(2\sqrt{q^2+k_0^2(T)})$, where $k_0(T)$ is the finite temperature analogy of the 2D Fermi wave vector. Yurtsever *et al.* [14] go further in that they formulate a dynamic local field correction, $G(\mathbf{q},\omega,T)$, within a qSTLS mean field theory framework inputted with the temperature-dependent Hartree-Fock structure function (see Ref. [24] for the temperature-dependent Lindhard function) to make their calculation more tractable; the approximation scheme of Ref. [14] is, in effect, a dynamical version of the static Hubbard approximation to the local field correction. The 2D plasmon dispersion curves that result from the latter two theoretical approaches are in very good agreement with the experimental data [16,17].

Turning now to the strong coupling regime, it has been known [5,7] for quite some time that the long-wavelength ($q\rightarrow 0$) plasmon dispersion in strongly coupled [$\Gamma=Z^2e^2/(\varepsilon_s a k_B T)\gg 1$] 2D classical electron liquids is entirely controlled by the potential energy part of the third-frequency-moment ($\langle\omega^3\rangle$) sum rule coefficient [see Eqs. (7) and (12) below] [4], which requires that, in the $\Gamma\rightarrow\infty$ limit, the plasmon dispersion approach the 2D hexagonal lattice [25] phonon frequency,

$$\omega_P(q\rightarrow 0)|_{T=0}^{\mathrm{CRYSTAL}}=\omega_{2\mathrm{D}}(q)[1-0.173qa]; \qquad (1)$$

$\omega_{2\mathrm{D}}(q)=\sqrt{2\pi ne^2q/m}$ is the 2D plasma frequency. The same should hold for the zero-temperature 2D quantum electron liquid in the $r_s\rightarrow\infty$ limit. Out of the approximation schemes listed above, only the Ref. [4] high-frequency sum rule expansion [Q(i)] satisfies this criterion. The resulting plasmon (P) frequency can be calculated with the aid of the Ref. [26] fitted Monte Carlo (MC) formula (14) for the correlation energy. One obtains

$$\omega_P(q\rightarrow 0)|_{r_s\rightarrow\infty}=\omega_{2\mathrm{D}}(q)[1-0.1694qa], \qquad (2)$$

which is in near agreement with the phonon dispersion formula above. As to the STLS approximation scheme [Q(iii)], the plasmon frequency

$$\omega_P(q\rightarrow 0)|_{r_s\rightarrow\infty}^{\mathrm{STLS}}=\omega_{2\mathrm{D}}(q)[1-0.2711qa]$$

does not even come close to reproducing the correct long-wavelength 2D Wigner crystal dispersion (1) in the $r_s\rightarrow\infty$ limit. The Hubbard approximation [Q(ii)] [1] underlying the Ref. [13] calculation, in fact, does with a coefficient 0.177 in Eq. (2). However, we believe this is coincidental. Moreover, the Hubbard approximation, because it is r_s independent, leads to the obviously false conclusion that the non-RPA correction is always the same for any r_s.

While the qSTLS treatment of Moudgil *et al.* [10] fails to reproduce the exchange-correlation part of the third-frequency-moment sum rule in the high-frequency limit, the inaccuracies that accrue in their description of the plasmon dispersion may be somewhat mitigated by the fact that these calculations address the weak coupling regime $r_s\leqslant 3$. As to the more involved iterative quantum kinetic theory treatment of Neilson *et al.* [6], which does provide plasmon dispersion results in the strong coupling regime $5\leqslant r_s\leqslant 40$, it is by no means clear that the exchange-correlation part of the $\langle\omega^3\rangle$ sum rule coefficient can be recovered from their formalism in the high-frequency limit.

The present work addresses the problem of constructing a dielectric function for the 2D electron liquid based on a physically correct microscopic model that, at the same time, correctly represents the behavior of $\varepsilon(\mathbf{q},\omega)$ in the strong coupling regime. To realize this goal, we invoke the quasilocalized charge approximation (QLCA), an approximation method that has proved to be consistently successful in the description of collective mode dispersion in strongly coupled classical Coulomb liquids as evidenced by comparison with a series of MD simulations [11,21,22,27,28]; we contend that the QLCA can be extended in a way that makes it suitable for the description of collective mode dispersion in the quantum domain.

The QLCA was formulated by two of the authors some time ago [11,19] for the purpose of describing collective mode dispersion in a variety of classical Coulomb liquid configurations [11,19,29–31] in the strong coupling regime. The basis of the formal development of the QLCA is that the dominating feature of the physical state of the plasma with $\Gamma\gg 1$ is the quasilocalization of the charges. This physical picture suggests a microscopic equation-of-motion model where the particles are trapped in local potential fluctuations. The particles occupy randomly located (but certainly not uncorrelated) sites and undergo oscillations around them. At the same time, however, the site positions also change and a continuous rearrangement of the underlying quasiequilibrium configuration takes place. Inherent in the QLC model is the assumption that the two time scales are well separated and that for the description of the rapid oscillating motion, the time average (converted into ensemble average) of the drifting quasiequilibrium configuration is sufficient. For this condition to be satisfied, it is necessary that the amplitude of the excursion of the oscillations be much smaller than the Wigner-Seitz radius; in Ref. [19] this is indeed shown to be the case provided that $\Gamma\gg 1$.

In the application of the QLCA to a strongly coupled charged-particle system in the quantum domain, the main physical difference one should consider between the classical and quantum behaviors is that in the latter the correlation-induced localization is hampered by the increase in kinetic energy that acts counter to the localization. Nevertheless, as it will be shown below, the QLCA meets the stated objective to the extent that it reproduces the exchange-correlation contribution to the $\langle\omega^3\rangle$ sum rule coefficient, thereby guaranteeing recovery of the correct oscillation frequency for arbitrary q values in the $r_s\rightarrow\infty$ limit. What the QLCA fails to reproduce is the correlational increase of the kinetic energy discussed above. This is a problem, however, only for intermediate r_s values: as $r_s\rightarrow\infty$, both the free-particle and correlation contributions to the kinetic energy part [see Eqs. (10) and (11) below] drop off like $1/r_s^2$ and $1/r_s^{3/2}$, respectively, while the dominant $O(1/r_s)$ correlation and Hartree-Fock exchange energy contributions to the interaction energy part [see Eqs. (6), (10), and (12) below] of the $\langle\omega^3\rangle$ sum rule coefficient add to give the Madelung energy as $O(1/r_s)$.

It is interesting to note that what one finds at zero temperature, namely that the softening of the plasmon dispersion by exchange correlation is partially offset by the average kinetic energy, is not dissimilar to the cancellation at finite temperatures between the temperature enhanced kinetic energy and correlation effects [13,17]. In the present work, we will, with reference to relevant experimental data [17], demonstrate that, in the strong coupling regime, it is the third-frequency-moment ($\langle\omega^3\rangle$) sum rule coefficient containing these two competing effects that plays the central role in the 2D plasmon dispersion at finite-q values.

The paper is organized in four sections. In Sec. II, we develop the dielectric response function, $\varepsilon(\mathbf{q},\omega)$, for strongly coupled 2D Coulomb liquids in the zero-temperature quantum domain. In Sec. III, we calculate the finite-q plasmon dispersion from the zeros of $\varepsilon(\mathbf{q},\omega)$ using available quantum MC data for the pair distribution function [26]. We will then compare the resulting finite-q theoretical plasmon dispersion curves with relevant Ref. [17] experimental data, and we will analyze the role the correlational part of the kinetic energy plays in the dispersion via the $\langle\omega^3\rangle$ sum rule coefficient. Conclusions are drawn in Sec. IV.

II. DIELECTRIC RESPONSE FUNCTION

In this section, we formulate the dielectric response function for the description of collective mode dispersion in strongly coupled 2D Coulomb liquids at zero-temperature in the normal fluid phase. The starting point for the development is the classical (cl) dielectric function that results from the QLCA,

$$\varepsilon(\mathbf{q},\omega)|_{\mathrm{cl}} = 1 - \frac{\phi_{2\mathrm{D}}(q)[nq^2/m\omega^2]}{1+\phi_{2\mathrm{D}}(q)[nq^2/m\omega^2]G_{\mathrm{QLCA}}(\mathbf{q})}. \quad (3)$$

Equation (3) is derived from the microscopic equation of motion for the collective coordinates $\xi_{\mathbf{q}}$, defined through the Fourier representation $\xi_i(t)=(1/\sqrt{Nm})\Sigma_{\mathbf{q}}\xi_{\mathbf{q}}(t)\exp(i\mathbf{q}\cdot\mathbf{x}_i)$ relating $\xi_{\mathbf{q}}$ to the ith-particle displacement ξ_i; see Refs. [11,19] for the details.

The QLCA static local field correction in Eq. (3),

$$G(\mathbf{q}) = -\frac{1}{N}\sum_{\mathbf{q}'}\frac{(\mathbf{q}\cdot\mathbf{q}')^2}{q^3q'}[S(|\mathbf{q}-\mathbf{q}'|)-S(q')] \quad (4a)$$

$$= 1 - \frac{1}{2q}\int_0^\infty dr\frac{1}{r^2}g(r)\left[1-4J_0(qr)+6\frac{J_1(qr)}{qr}\right], \quad (4b)$$

is expressed in terms of static structure functions $S(q)$, or, equivalently, in terms of the pair distribution function

$$g(r) = 1 - \frac{1}{N}\sum_{\mathbf{q}}[1-S(q)]\exp(i\mathbf{q}\cdot\mathbf{r}). \quad (5)$$

At long wavelengths, (4) simplifies to

$$G(q\to 0) = \frac{5}{16}\frac{|\langle V\rangle|}{(e^2/a)}qa; \quad (6)$$

$$\langle V\rangle = \frac{1}{2A}\sum_{\mathbf{q}}\phi_{2\mathrm{D}}(q)[S(q)-1] \quad (7)$$

is the potential energy per particle. The derivation of Eq. (3) is predicated on the assumption that thermal motions are negligible: this is a reasonable assumption for a classical charged-particle system in the strong coupling regime where the potential energy dominates. In contrast, for a degenerate system, this certainly is not the case and one should therefore take account of the equilibrium momenta of the particles. In Eq. (3), the $nq^2/(m\omega^2)$ factor is readily identified as the Vlasov density response function for momentum distribution function $f(\mathbf{p})\sim n\delta(\mathbf{p})$. One may therefore assume that for a Fermi distribution of momenta, the appropriate replacement for $nq^2/(m\omega^2)$ is the Lindhard function

$$\chi_0(\mathbf{q},\omega) = \frac{2}{\hbar A}\sum_{\mathbf{p}}\frac{f(|\mathbf{p}+(1/2)\mathbf{q}|)-f(|\mathbf{p}-(1/2)\mathbf{q}|)}{\omega+(\hbar/m)\mathbf{p}\cdot\mathbf{q}+i\eta}, \quad (8)$$

and the resulting dielectric response function takes the familiar form

$$\varepsilon(\mathbf{q},\omega) = 1 - \frac{\phi_{2\mathrm{D}}(q)\chi_0(\mathbf{q},\omega)}{1+\phi_{2\mathrm{D}}(q)\chi_0(\mathbf{q},\omega)G(\mathbf{q})}. \quad (9)$$

The local field factor in Eq. (9) is formally identical to the $G(\mathbf{q})$in Eq. (4), but it should be borne in mind that $g(r)$ is now the pair distribution function appropriate for the 2D zero-temperature electron liquid in the normal fluid phase (as determined, e.g., by Tanatar and Ceperley [26]) and as such, it embodies all the exchange-correlation effects. Consequently, the $\varepsilon(\mathbf{q},\omega)$ of Eq. (9) now satisfies, to leading order in r_s, the third-frequency-moment sum rule with coefficient

$$\langle\omega^3\rangle(\mathbf{q}) = \frac{1}{\pi\phi_{2\mathrm{D}}(q)}\int_{-\infty}^{\infty}d\omega\,\omega^3\,\mathrm{Im}\frac{1}{\varepsilon(\mathbf{q},\omega)}$$
$$= -\frac{nq^2}{m}\left\{\omega_{2\mathrm{D}}^2(q)[1-G(\mathbf{q})]+\frac{3q^2}{m}\langle E_{\mathrm{kin}}\rangle+\left[\frac{\hbar q^2}{2m}\right]^2\right\}, \quad (10)$$

$\langle E_{\mathrm{kin}}\rangle = e^2\varepsilon_{\mathrm{kin}}/(2a_B)$ is the expectation value of the kinetic energy per particle for the *interacting* system consisting of a noninteracting (0) part and a correlational (c) part,

$$\varepsilon_{\mathrm{kin}} = \varepsilon_{\mathrm{kin}}^0 + \varepsilon_{\mathrm{kin}}^c,$$

$$\varepsilon_{\mathrm{kin}}^0 = \frac{1}{r_s^2},\quad \varepsilon_{\mathrm{kin}}^c = -\frac{\partial}{\partial r_s}(r_s\varepsilon_c), \quad (11)$$

$\varepsilon_{\mathrm{kin}}$ and ε_c are the kinetic and the correlation energies per particle in Rydberg units. Note that the leading contribution to ε_c drops off like $1/r_s$, whereas $\varepsilon_{\mathrm{kin}}^c$ drops off like $1/r_s^{3/2}$. We also note that $\langle V\rangle = e^2\varepsilon_{\mathrm{int}}/(2a_B)$ of Eq. (7), now represents the total interaction energy consisting of the Hartree-Fock exchange and potential energy contributions,

$$\varepsilon_{\mathrm{int}} = \varepsilon_{\mathrm{ex}} + \varepsilon_{\mathrm{pot}},$$

$$\varepsilon_{\rm ex} = -\frac{8\sqrt{2}}{3\pi r_s}, \quad \varepsilon_{\rm pot} = \frac{1}{r_s}\frac{\partial}{\partial r_s}(r_s^2 \varepsilon_c) \ \ ({\rm Ryd}). \tag{12}$$

As a reminder, the ground-state energy per particle, $\varepsilon_{\rm total}$, can be written as

$$\varepsilon_{\rm total} = \varepsilon_{\rm kin}^0 + \varepsilon_{\rm ex} + \varepsilon_c = \varepsilon_{\rm kin} + \varepsilon_{\rm int}. \tag{13}$$

Going beyond the leading order in r_s, the dielectric function (9) cannot reproduce the correlational part, $\varepsilon_{\rm kin}^c$, of the kinetic energy contribution (11) to the sum rule coefficient (10) (in contrast to the classical regime where the kinetic energy is unaffected by particle correlations, i.e., $\langle E_{\rm kin}\rangle = k_B T$).

Finally, we note that Eq. (4) is consistent with the $q \to \infty$ limit of the Kimball identity [32],

$$\lim_{q\to\infty}[1 - G(\mathbf{q})] = g(r=0), \tag{14}$$

valid for any static local field correction $G(\mathbf{q})$ that one may use to approximate the exact $G(\mathbf{q},\omega)$ for all values of ω.

III. COLLECTIVE MODE DISPERSION

We turn now to the calculation of collective mode dispersion in the 2D degenerate electron liquid in the strong coupling regime. For the zero-temperature $\chi_0(\mathbf{q},\omega)$ in (9), we use the results of Stern [33] and Isihara [34]. The mode frequency in the region $\bar{\omega} \geq 2\bar{q} + \bar{q}^2$ above the left boundary of the pair continuum is obtained by equating to zero the dielectric response function (9) with $\chi_0(\mathbf{q},\omega)$ given by [33,34]

$$\chi_0(\mathbf{q},\omega) = -\frac{m}{\pi\hbar^2}\left\{1 + \frac{1}{2\bar{q}^2}\left[\sqrt{(\bar{\omega}-\bar{q}^2)^2 - 4\bar{q}^2} - \sqrt{(\bar{\omega}+\bar{q}^2)^2 - 4\bar{q}^2}\right]\right\}. \tag{15}$$

At long wavelengths, we obtain

$$\frac{\omega_P(q\to 0)}{\omega_{\rm 2D}(q)} = 1 + \frac{3r_s}{8}\varepsilon_{\rm kin}^0 qa + \frac{5r_s}{64}\varepsilon_{\rm int} qa. \tag{16}$$

The third right-hand-side member is the part originating from $G(q\to 0)$ given by Eqs. (6) and (12). As has been pointed out above, the correlational part of the kinetic energy [represented by the second right-hand-side member of Eq. (11)] is missing from $G(\mathbf{q})$; the same defect shows up in Eq. (16). Since this last contribution would act to *increase* the kinetic energy, Eq. (16) evidently overestimates the depression (softening) of the dispersion curve that arises from the effect of exchange and correlations. In the $q\to 0$ domain, with the aid of the Ref. [26] MC fitted formula (14) for the correlation energy, we calculate this overestimate to be approximately 30% at $r_s = 20$, decreasing to 23% at $r_s = 40$. In the $r_s \to \infty$ limit, where the total kinetic energy ceases to contribute to the small-q dispersion, one recovers Eq. (2) from the oscillation frequency (16).

For the analysis of the plasmon dispersion at finite-q values, it is convenient to introduce the dimensionless quantities

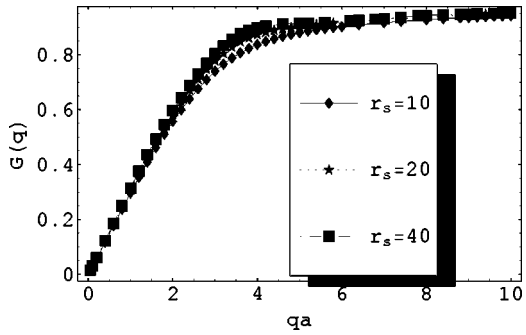

FIG. 1. Static local field correction, $G(q)$, as a function of qa for $r_s = 10, 20, 40$; $a = 1/\sqrt{\pi n}$. $G(q)$ is calculated from Eq. (4b) inputted with the Ref. [26] quantum Monte Carlo data for the pair distribution function $g(r)$.

$\bar{q} = q/k_F$ and $\bar{\omega} = \omega/\omega_F$, where $k_F = \sqrt{2\pi n}$ is the 2D Fermi wave number and $\hbar\omega_F = \varepsilon_F$. As is always the case whenever the random-phase approximation (RPA) is modified by a static local field correction, the dielectric function (9) does not take account of collisional (multipair excitations) damping, leaving Landau damping as the sole mechanism responsible for the decay of the collective excitations in the present study. At zero temperature, the Landau damping is confined to the pair continuum region of the $\bar{q}$, $\bar{\omega}$ plane. For $\bar{\omega} \geq 0$, the equations for the left and right boundaries of the continuum region are given by $\bar{\omega} = 2\bar{q} + \bar{q}^2$ and $\bar{\omega} = -2\bar{q} + \bar{q}^2$, respectively.

For a fixed value of r_s, $G(q)$ is calculated from Eq. (4b) with the input of the Ref. [26] quantum MC data for $g(r)$ of the 2D electron gas in the normal fluid phase; the resulting curves, displayed in Fig. 1 for $r_s = 10$, 20, 40, show $G(q)$ to be a monotonically increasing function ranging from zero to unity. To further check the accuracy of Fig. 1, independent calculations of $G(q\to 0)$ from Eqs. (6) and (12) using the Ref. [26] fitted MC formula (14) for the correlation energy show excellent agreement with Fig. 1 up to $qa \approx 1$.

The subsequent straightforward calculation of the plasmon oscillation frequency in the region $\bar{\omega} \geq 2\bar{q} + \bar{q}^2$, $\bar{q} \geq 0$ is then carried out by substituting the Lindhard density response function (15) into (9) and setting $\varepsilon(\bar{q},\bar{\omega}) = 0$. The resulting dispersion curves are displayed in Fig. 2 along with their RPA counterparts for $r_s = 10$, 20, and 40. Also shown in Fig. 2 are the most relevant experimental dispersion data available from Ref. [17] for $r_s = 15.2$, $T_F = 0.5393$ K, and $T = 0.25$ K. To make a meaningful comparison with the zero-temperature dispersion curves possible, we introduce the effective coupling parameter $r_s^* = r_s[1 - \exp(-T_F/T)]$. The justification for this choice follows from the fact that the compressibility sum rule for the 2D electron liquid is expressible in terms of r_s^* for any temperature [35]. With this replacement, we assign the calculated $r_s^* = 13.44$ value to the Fig. 2 data points. As a result, we find a fair, but by no means exact, agreement between theory and experiment with the data points lying close to the $r_s = 20$ curve.

In order to try to understand the origin of this discrepancy, we re-calculate the plasmon dispersion per the prescription of Ref. [4] with the local field factor $G(\mathbf{q})$ in Eq. (9) replaced by a tentative local field factor, $\tilde{G}(\mathbf{q})$, that accounts for the

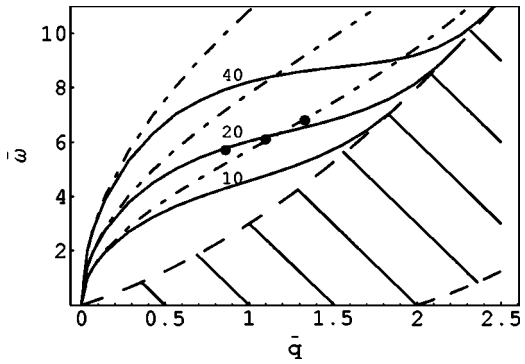

FIG. 2. Plasmon dispersion curves for $r_s=10,20,40$ in the region $\bar{\omega}\geqslant 2\bar{q}+\bar{q}^2$ above the left boundary of the RPA pair continuum region (hachured); $\bar{q}=q/k_F$, $\bar{\omega}=\omega/\omega_F$; $k_F=\sqrt{2\pi n}$, $\hbar\omega_F=\varepsilon_F=\pi n\hbar^2/m$. The solid curves are calculated from Eqs. (9) and (15), with $G(q)$ calculated from (4b) using the Ref. [26] quantum Monte Carlo (MC) data for the pair distribution function, $g(r)$, of the electron gas in the normal fluid phase. The dashed RPA curves are calculated from Eq. (9) with $G(q)$ set equal to zero. The Ref. [17] experimental data points (solid circles) correspond to an effective $r_s^*=13.44$.

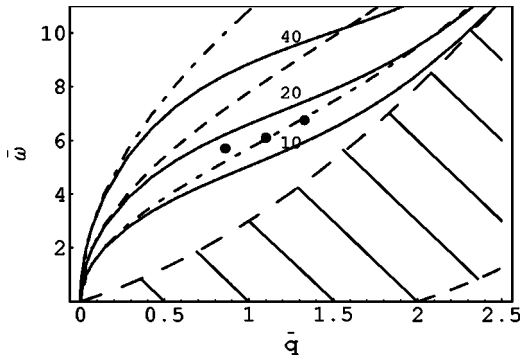

FIG. 3. Plasmon dispersion curves for $r_s=10,20,40$ in the region $\bar{\omega}\geqslant 2\bar{q}+\bar{q}^2$ above the left boundary of the RPA pair continuum region (hachured). The solid curves are calculated from Eqs. (9) and (15), with $\tilde{G}(\mathbf{q})$ calculated from (17) and (4b) using the Ref. [26] QMC data for $g(r)$ in the normal fluid phase and the Ref. [26] MC fitted formula (14) for the correlation energy per particle; $\tilde{G}(\mathbf{q})$ replaces $G(\mathbf{q})$ in (9). The dashed RPA $[G(\mathbf{q})=0]$ curves are calculated from Eq. (9) with $G(q)$ set equal to zero. The Ref. [17] experimental data points (solid circles) correspond to an effective $r_s^*=13.44$.

missing correlational part of the kinetic energy, in full compliance with the third-frequency-moment sum rule:

$$\tilde{G}(\mathbf{q})=G(\mathbf{q})-\frac{3r_s}{2\sqrt{2}}\varepsilon_{\mathrm{kin}}^{c}\bar{q}. \tag{17}$$

It should be noted that Eq. (17) in fact represents $G(\mathbf{q},\omega\rightarrow\infty)$ since it is derived from the high-frequency sum rule and, as such, should provide a correct representation of $\varepsilon(\mathbf{q},\omega)$ and the plasmon dispersion relation in that limit. In contrast, other representations of the local field factor with the inclusion of the correlational part of the kinetic energy term [36,37], where this latter term appears with the opposite sign and a different numerical coefficient, correspond to $G(\mathbf{q},\omega=0)$ appropriate only for the analysis of static properties. For a comprehensive discussion of this issue, see Ref. [37].

Should we consider the behavior of $\tilde{G}(\mathbf{q})$ for $q\rightarrow\infty$, the linear structure of the correction term in (17) would have to break down in order to ensure compliance with the Rajagopal-Kimball identity (14), with the correlational part of the kinetic energy appearing in a different guise in the local field factor. We may, however, assume that the representation (17) reasonably well approximates the static local field factor up to $\bar{q}\approx 1.5$. Then calculating ε_c and its first derivative with respect to r_s from the Ref. [26] fitted MC formula (14), we can generate amended dispersion curves from Eq. (17). These are displayed in Fig. 3. Now, we observe that the same $r_s^*=13.44$ experimental data points lie between the $r_s=10$, 20 theory curves. This supports our claim that in the strong coupling (low density) regime, the plasmon dispersion is entirely controlled by the competing exchange-correlation and kinetic energy effects in the third-frequency-moment sum rule coefficient. At long wavelengths, the combination of Eqs. (6) and (17) with (9) and (15) necessarily provides

$$\frac{\omega_P(q\rightarrow 0)}{\omega_{2\mathrm{D}}(q)}=1+\frac{3r_s}{8}\varepsilon_{\mathrm{kin}}qa+\frac{5r_s}{64}\varepsilon_{\mathrm{int}}qa, \tag{18}$$

in agreement with the plasmon frequency calculated by Iwamoto *et al.* [4] from the high-frequency sum rule expansion. Note the difference between the kinetic energy terms in Eqs. (18) and (16). Substituting the Ref. [26] fitted MC formula (14) for the correlation energy into Eq. (18), our calculations indicate that (i) at $r_s=10$, the kinetic energy overwhelms the softening effect of the potential energy, $\varepsilon_{\mathrm{pot}}$, on the plasmon dispersion; (ii) at $r_s=20$, the kinetic energy and potential energy contributions cancel each other leaving only the exchange to soften the plasmon dispersion; (iii) however, at $r_s=40$, only a portion of the potential energy is cancelled by the kinetic energy. Note that the $r_s=40$ dispersion curve that has been included in Figs. 2 and 3, mostly for illustrative purposes, represents in a way an unstable liquid phase since the transition to a 2D Wigner crystal is believed to occur at $r_s=37$.

In a strongly coupled Coulomb liquid, for sufficiently high coupling, the isothermal compressibility becomes negative. As a result, the static dielectric response function, $\varepsilon(\bar{q},0)$, also becomes negative somewhere in the interval $0<\bar{q}<\bar{q}_0$, where $\bar{q}_0$ is in the vicinity of or greater than the reciprocal lattice vector of the incipient Wigner lattice and $\varepsilon(\bar{q},0)$ develops poles both at $\bar{q}=0$ and at $\bar{q}=\bar{q}_0$. (For a classical 2D OCP, see Ref. [38] and for the 3D electron gas, see Ref. [39].) This latter pole is expected to survive for $\varepsilon(\bar{q},\bar{\omega})$ dynamical. Now, it is known that the appearance of a pole in $\varepsilon(\bar{q},\bar{\omega})$ is the indicator of a resonance in the single-particle dynamical spectrum and, as such, can have a profound effect on the collective mode dispersion (as borne out, for example, by the well-known cyclotron resonance in magnetized plasmas). In order to identify this pole in the case of the 2D zero-temperature Coulomb liquid, we analyze $\varepsilon(\bar{q},\bar{\omega})$ in the

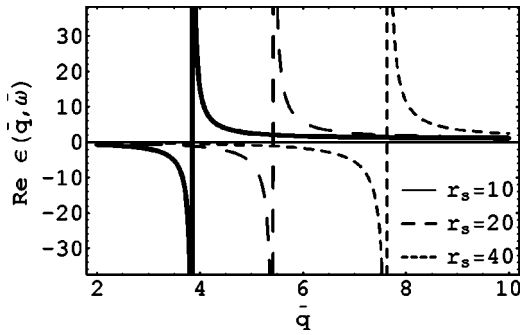

FIG. 4. Re $\varepsilon(\bar{q},\bar{\omega})$ as a function of $\bar{q}$ on the right boundary, $\bar{\omega}=-2\bar{q}+\bar{q}^2$, of the continuum region. Note the rightward progression of the vertical asymptote along the boundary as r_s increases from 10 to 40.

region $0\leqslant\bar{\omega}\leqslant-2\bar{q}+\bar{q}^2$, $\bar{q}\geqslant 2$ below the right boundary of the pair continuum, where [33,34]

$$\chi_0(\mathbf{q},\omega)=-\frac{m}{\pi\hbar^2}\left\{1-\frac{1}{2\bar{q}^2}[\sqrt{(\bar{\omega}-\bar{q}^2)^2-4\bar{q}^2}+\sqrt{(\bar{\omega}+\bar{q}^2)^2-4\bar{q}^2}]\right\}. \tag{19}$$

From (19), we observe that $\chi_0(\bar{q},\bar{\omega}=-2\bar{q}+\bar{q}^2)$ is always negative on the right boundary of the pair continuum. Then according to (9), $\varepsilon(\bar{q},-2\bar{q}+\bar{q}^2)$ has a discontinuity at some $\bar{q}$, say $\bar{q}_*(r_s)$, where its denominator $1+\phi_{2D}(q)\chi_0(\bar{q},-2\bar{q}+\bar{q}^2)G(\bar{q})$ is zero. The location of the vertical asymptote of the discontinuity at $\bar{q}_*(r_s)$, is shown in Fig. 4. Its continuation as first-order poles into the $0\leqslant\bar{\omega}<-2\bar{q}+\bar{q}^2$, $\bar{q}\geqslant 2$ domain (portrayed by Fig. 5) is a consequence of the fact that $\chi_0(\mathbf{q},\omega)$ remains negative throughout that entire domain. For a given r_s, the locus $\bar{\omega}_*(\bar{q})$ of all such poles from $\bar{\omega}_*=0$ up to the right boundary $\bar{\omega}_*=-2\bar{q}_*+\bar{q}_*^2$ then forms the family of curves shown in Fig. 6. Evidently, the total charge density perturbation is perfectly screened for these q,ω values. Further analysis shows that the poles persist for r_s values all the way down to $\sqrt{2}/G(\bar{q}=2)\approx 1.96$. This critical value compares favorably with the Hartree-Fock $r_s=\pi/\sqrt{2}=2.22$ prediction [40,41], and with the MC $r_s\sim 2.03$ value [26] and experimentally observed value $r_s=1.71$ [41] for the onset of negative compressibility. Note that while the location of the poles is contingent upon the structure of the chosen local field $G(\bar{q})$, their very existence is not particularly sensitive to this choice: any positive $G(\mathbf{q})$ will lead to the same kind of discontinuity in the dielectric response function.

We may now conjecture that the existence of the resonance leads to the emergence of a new collective excitation, to be referred to in the sequel as the high-q mode. The analogy with the cyclotron resonance again can be usefully invoked: there, the resonance at the cyclotron frequency ω_c leads to the upper hybrid frequency $\omega_U=\sqrt{\omega_{2D}^2(q)+\omega_c^2}$, a collective excitation generated by the coupling of ω_c to the plasma frequency $\omega_{2D}(q)$.

To clarify the physical origin of the conjectured excitation, we suggest that the governing mechanism is related to

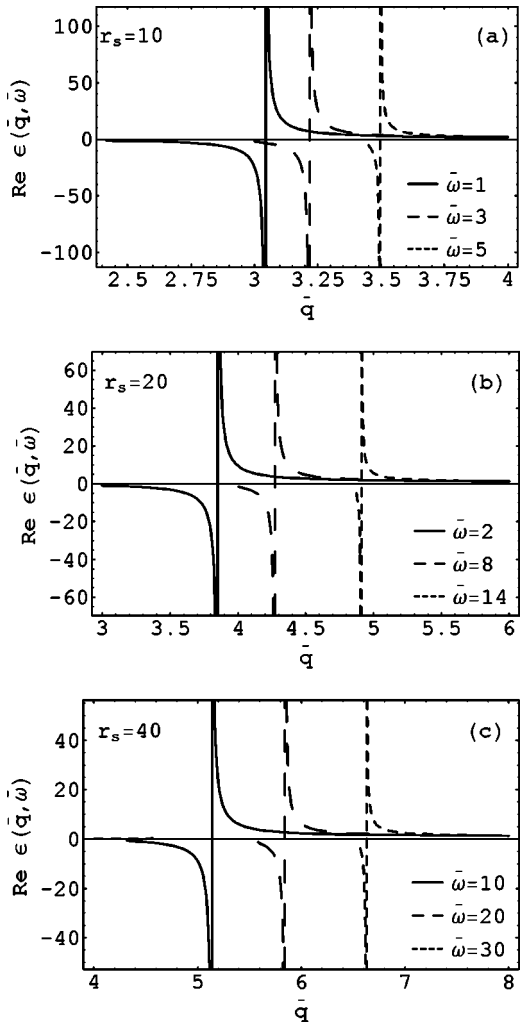

FIG. 5. In the region $0\leqslant\bar{\omega}\leqslant-2\bar{q}+\bar{q}^2$, $\bar{q}\geqslant 2$: Re $\varepsilon(\bar{q},\bar{\omega})$ as a function of $\bar{q}$ for the three indicated values of $\bar{\omega}$ in each of the three graphs. Note the rightward progression of the vertical asymptote with increasing $\bar{\omega}$. (a) $r_s=10$, (b) $r_s=20$, (c) $r_s=40$.

the fact that the existence of the pole in $\varepsilon(\bar{q},0)$ at $\bar{q}=\bar{q}_0$ is indicative of the system's propensity to develop a charge-density wave (CDW) with a wave number in the vicinity of $\bar{q}_0$. While a CDW does not develop for an OCP in the static

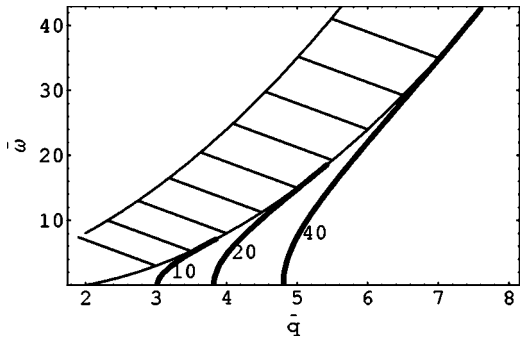

FIG. 6. In the region $0\leqslant\bar{\omega}\leqslant-2\bar{q}+\bar{q}^2$, $\bar{q}\geqslant 2$: Loci of first-order poles of the dielectric response function, $\varepsilon(\bar{q},\bar{\omega})$, for $r_s=10,20,40$ calculated from Eqs. (9), (4b), and (19) and inferred from Figs. 4 and 5.

limit, it can be brought into existence by the introduction of a second species of (weakly correlated) charges which can provide an additional static screening. A similar situation seems to arise once dynamical behavior is considered. When a traveling periodic potential develops at this wave number, then it is the motion of the particles in the troughs of this potential that is responsible for the appearance of the single-particle frequency $\overline{\omega}_*(\overline{q};r_s)$, the generator of the high-q mode. While it is unclear that this excitation would develop in an OCP, our preliminary analysis indicates that, in the presence of a second component, an undamped high-q excitation would develop in close proximity to the right boundary of the pair continuum. It should be noted that the proposed scenario is appropriate only in the liquid phase: both strong coupling (absent in the gaseous phase) and particle mobility (absent in the solid phase) are needed to support the underlying dynamics.

IV. CONCLUSIONS

In this paper, we have analyzed the longitudinal collective mode dispersion in strongly coupled ($r_s \gg 1$) 2D Coulomb liquids at zero temperature. The analysis is based on an extension of the classical quasilocalized charge approximation (QLCA) [11,19] into the quantum domain. The basis of the formal microscopic development of the QLCA is that the dominating feature of the physical state of strongly coupled Coulomb liquids is the quasilocalization of the charges. The static local field factor, $G(\mathbf{q})$, given by (4a) and (4b), satisfies the Rajagopal-Kimball condition (14) for any r_s value and the Eq. (9) dielectric response function, $\varepsilon(\mathbf{q},\omega)$, satisfies the third-frequency-moment sum rule in the $r_s \to \infty$ limit. For finite r_s values, however, $\varepsilon(\mathbf{q},\omega)$ fails to reproduce the correlational part of the kinetic energy in the $\langle \omega^3 \rangle$ sum rule coefficient. The dispersion relation derived from $\varepsilon(\mathbf{q},\omega)$ is in fair qualitative agreement with recent experimental results [17]. The agreement is improved by an *ad hoc* addition of the correlational part of the kinetic energy to $G(\mathbf{q})$. In evaluating the local field factor, we have used the pair distribution function and correlation energy quantum Monte Carlo data from Ref. [26]. The numerical results for the improved dispersion curves are in very good agreement with the inelastic light-scattering data of Ref. [17].

While other theories [13,14] have recently been put forward to provide the theoretical underpinnings of the Refs. [14,16] experimental results, the present work is the only approach to collective mode dispersion having both a microscopic basis and a rigorous compliance with the two high-frequency sum rules in the $r_s \to \infty$ limit.

An unexpected result emerging from our analysis is the possible existence of a new high-q longitudinal collective excitation in close proximity to the right boundary of the pair continuum. The physical origin of this excitation seems to originate from the negative compressibilty and the associated dynamical charge-density wave that develops in strongly coupled two-component Coulomb liquids for sufficiently high coupling values.

ACKNOWLEDGMENTS

This material is based upon work supported by the National Science Foundation and the Department of Energy under Grant Nos. PHY-0206554, PHY-0206695, and DE-FG02-98ER54501. The participation of one of the authors (H.M.) in this research was also partially sponsored by the Vermont Space Grant Consortium and by NASA under Grant No. NGT5-40110. One of the authors (G.J.K.) gratefully acknowledges discussions with Marlene Rosenberg and Stamatios Kyrkos. Two of the authors (K.I.G. and G.J.K.) acknowledge useful discussions with Gaetano Senatore.

[1] M. Jonson, J. Phys. C **9**, 3055 (1976).
[2] M. Baus, J. Stat. Phys. **19**, 163 (1978).
[3] N. Studart and O. Hipolito, Phys. Rev. A **22**, 2860 (1980).
[4] N. Iwamoto, E. Krotscheck, and D. Pines, Phys. Rev. B **29**, 3936 (1984); N. Iwamoto Phys. Rev. A **30**, 3289 (1984).
[5] K. I. Golden and De-xin Lu, Phys. Rev. A **31**, 1763 (1985).
[6] D. Neilson, L. Swierkowski, A. Sjolander, and J. Szymanski, Phys. Rev. B **44**, 6291 (1991).
[7] K. I. Golden, G. Kalman, and Ph. Wyns, Phys. Rev. A **41**, 6940 (1990); **46**, 3463 (1992).
[8] A. Gold and L. Calmels, Phys. Rev. B **48**, 11622 (1993).
[9] R. K. Moudgil, P. K. Ahluwalia, and K. N. Pathak, Phys. Rev. B **51**, 1575 (1995).
[10] R. K. Moudgil, P. K. Ahluwalia, and K. N. Pathak, Phys. Rev. B **52**, 11945 (1995).
[11] K. I. Golden and G. Kalman, Phys. Plasmas **7**, 14 (2000).
[12] M. P. Das, K. I. Golden, and F. Green, Phys. Rev. E **64**, 046125 (2001).
[13] E. H. Hwang and S. Das Sarma, Phys. Rev. B **64**, 165409 (2001).
[14] A. Yurtsever, V. Moldoveanu, and B. Tanatar, Phys. Rev. B **67**, 115308 (2003).
[15] G. S. Atwal, I. G. Khalil, and N. W. Ashcroft, Phys. Rev. B **67**, 115107 (2003).
[16] M. A. Eriksson, A. Pinczuk, B. S. Dennis, C. F. Hirjibehedin, S. H. Simon, L. N. Pfeiffer, and K. W. West, Physica E (Amsterdam) **6**, 165 (2000).
[17] C. F. Hirjibehedin, A. Pinczuk, B. S. Dennis, L. N. Pfeiffer, and K. W. West, Phys. Rev. B **65**, 161309 (2002).
[18] K. S. Singwi, M. P. Tosi, R. H. Land, and A. Sjolander, Phys. Rev. **176**, 589 (1968); K. S. Singwi, A. Sjolander, M. P. Tosi, and R. H. Land, Solid State Commun. **7**, 1503 (1969); Phys. Rev. B **1**, 1044 (1970); P. Vashishta and K. S. Singwi, *ibid.* **6**, 875 (1972).
[19] G. Kalman and K. I. Golden, Phys. Rev. A **41**, 5516 (1990).
[20] K. I. Golden and G. Kalman, Phys. Rev. A **19**, 2112 (1979).
[21] H. Totsuji and H. Kakeya, Phys. Rev. A **22**, 1220 (1980).
[22] G. J. Kalman, P. Hartmann, Z. Donko, and M. Rosenberg, Phys. Rev. Lett. **92**, 065001 (2004).
[23] G. Niklasson, Phys. Rev. B **10**, 3052 (1974); T. Hasegawa and M. Shimizu, J. Phys. Soc. Jpn. **38**, 965 (1975); **39**, 569 (1975).

[24] P. F. Maldague, Surf. Sci. **73**, 296 (1978).
[25] L. Bonsall and A. A. Maradudin, Phys. Rev. B **15**, 1959 (1977).
[26] B. Tanatar and D. M. Ceperley, Phys. Rev. B **39**, 5005 (1989).
[27] P. Schmidt, G. Zwicknagel, P.-G. Reinhard, and C. Toepffer, Phys. Rev. E **56**, 7310 (1997).
[28] Z. Donko, G. J. Kalman, P. Hartmann, K. I. Golden, and K. Kutasi, Phys. Rev. Lett. **90**, 226804 (2003).
[29] K. I. Golden, G. Kalman, and Ph. Wyns, Phys. Rev. A **46**, 3454 (1992).
[30] K. I. Golden and G. Kalman, Phys. Status Solidi B **180**, 533 (1993).
[31] G. Kalman, V. Valtchinov, and K. I. Golden, Phys. Rev. Lett. **82**, 3124 (1999).
[32] J. C. Kimball, Phys. Rev. A **7**, 1648 (1973).
[33] F. Stern, Phys. Rev. Lett. **14**, 546 (1967); **30**, 278 (1973).
[34] A. Isihara, Solid State Phys. **42**, 271 (1988).
[35] K. I. Golden and G. Kalman, J. Phys. A **36**, 5865 (2003).
[36] B. Davoudi, M. Polini, G. F. Giuliani, and M. P. Tosi, Phys. Rev. B **64**, 153101 (2001).
[37] A. Holas, in *Strongly Coupled Plasma Physics*, edited by F. J. Rogers and H. E. DeWitt (Plenum, New York, 1986), pp. 463–482.
[38] S. Kyrkos and G. J. Kalman, J. Phys. A **36**, 6235 (2003).
[39] C. Bowen, G. Sugiyama, and B. J. Alder, Phys. Rev. B **50**, 14838 (1994); S. Moroni, D. M. Ceperley, and G. Senatore, Phys. Rev. Lett. **75**, 689 (1995).
[40] S. Ilani, A. Yacoby, D. Mahalu, and H. Shtrikman, Phys. Rev. Lett. **84**, 3133 (2000).
[41] J. P. Eisenstein, L. N. Pfeiffer, and K. W. West, Phys. Rev. Lett. **68**, 674 (1992); Phys. Rev. B **50**, 1760 (1994).